



13th World Conference on Earthquake Engineering
Vancouver, B.C., Canada
August 1-6, 2004
Paper No. 1463

INVESTIGATING THE INFLUENCE OF ELASTIC SPECTRAL SHAPE ON THE LIMIT-STATE CAPACITIES OF A 9-STORY BUILDING THROUGH IDA

Dimitrios VAMVATSIKOS¹ and C. Allin CORNELL²

SUMMARY

The influence of the elastic spectral shape on the limit-state capacities of a 9-story steel moment-resisting frame is investigated through the use of Incremental Dynamic Analysis (IDA). IDA is a parametric analysis method that has recently emerged to estimate more thoroughly structural performance under seismic loads. It involves subjecting a structural model to several ground motion records, each scaled to multiple levels of intensity (measured by the Intensity Measure, *IM*), thus producing curves of response parameterized versus intensity level, on top of which limit-states can be defined and corresponding capacities can be calculated. When traditional *IM*s, such as the peak ground acceleration or the 5%-damped first-mode spectral acceleration, are used, the *IM*-values of limit-state capacity can display large record-to-record variability. Thus, a large number of ground motion records has to be used to achieve a given level of confidence in the results. By testing a multitude of single spectral values as well as scalar combinations of spectral ordinates on the 9-story frame, several candidate *IM*s are found that significantly reduce such dispersion and consequently the needed number of records. Furthermore, such results are used to determine the most influential regions (or periods) of the elastic spectrum for each limit-state of the building. Thus, we are able to observe the evolution of such influential periods as the seismic intensity and the response of the building increase, from first yield all the way to global collapse. In conclusion, the ordinates of the elastic spectrum and the spectral shape of each individual record are found to significantly influence the seismic performance of the building and they are shown to provide promising candidates for new, more efficient *IM*s.

INTRODUCTION

An important aspect of Performance-Based Earthquake Engineering (PBEE) is calculating, for a given building, capacities for the limit-states of interest and their corresponding mean annual frequencies of exceedance. A promising method that has been developed to meet these needs is Incremental Dynamic Analysis (IDA). It involves performing nonlinear dynamic analyses of the structural model under a suite of ground motion records, each scaled to several intensity levels designed to force the structure all the way from elasticity to final global dynamic instability (Vamvatsikos [1]). Thus, we can generate IDA curves of the structural response, as measured by a Damage Measure (*DM*, e.g., peak roof drift ratio or the maximum peak interstory

¹ Theagenous 11, Athens 11634, Greece. E-mail: divamva@stanfordalumni.org

² Professor, Department of Civil and Environmental Engineering, Stanford University, CA 94305-4020

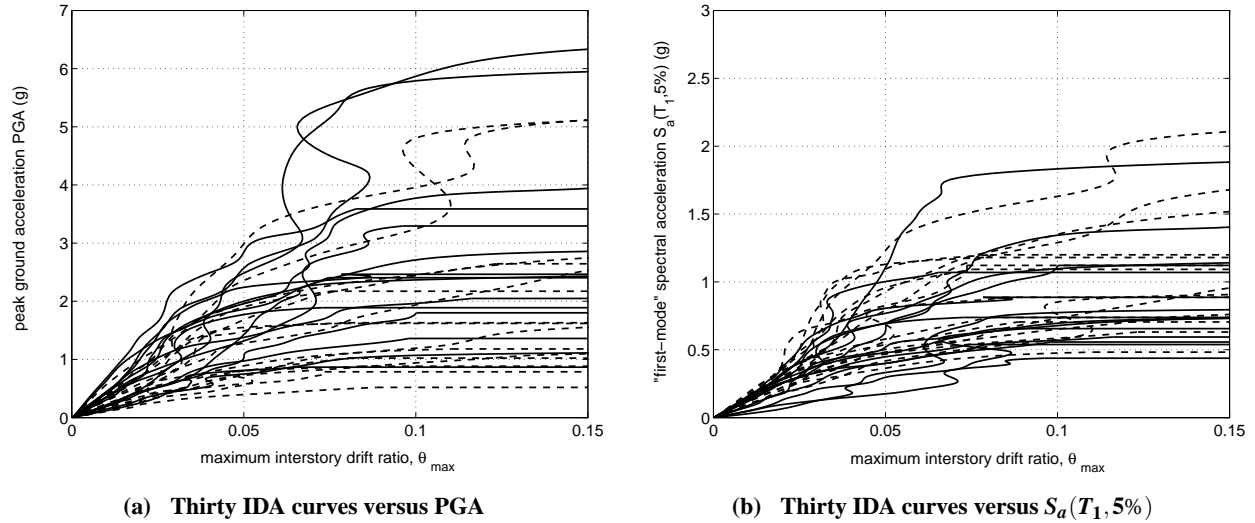


Figure 1. IDA curves for a $T_1 = 2.4s$, 9-story steel moment-resisting frame with fracturing connections plotted against (a) PGA and (b) $S_a(T_1, 5\%)$.

drift ratio θ_{\max}), versus the ground motion intensity level, measured by an Intensity Measure (*IM*, e.g., peak ground acceleration, PGA, or the 5%-damped first-mode spectral acceleration $S_a(T_1, 5\%)$). Subsequently, limit-states (e.g., Immediate Occupancy or Collapse Prevention in FEMA [2, 3]) can be defined on each IDA curve and the corresponding capacities can be calculated. The resulting capacities are then summarized, e.g., into appropriate fractile capacities, combined with probabilistic seismic hazard analysis results and integrated within a suitable PBEE framework to allow the calculation of the mean annual frequencies of exceeding each limit-state (Vamvatsikos [4]).

It is an unavoidable fact that the IDA curves and, correspondingly, the limit-state capacities display large record-to-record variability even for the simplest of structures, e.g., oscillators (Vamvatsikos [5]). This observed dispersion is closely connected to the *IM* used; some *IM*s are more *efficient* than others, better capturing and explaining the differences from record to record, thus bringing the results from all records closer together. Compare, for example, Figures 1a and 1b, where thirty IDA curves of a 9-story steel moment-resisting frame are plotted using PGA and $S_a(T_1, 5\%)$, respectively, as the *IM*. In both cases the variability from record to record is indeed remarkable, especially considering that the thirty records were chosen to represent a scenario earthquake and belong to a narrow magnitude and distance bin (Table 1). However, PGA (Figure 1a) is proven to be deficient relative to $S_a(T_1, 5\%)$ (Figure 1b) in expressing the limit-state capacities of the 9-story; it increases the variability between the curves and, correspondingly, the dispersion of capacities everywhere on the IDAs. On the other hand, even the improvement achieved by $S_a(T_1, 5\%)$ still leaves something to be desired, as dispersions remain in the order of 40% – 50%.

Why should we search for such a better *IM*? There is a clear computational advantage if we can select it *a priori*, before the IDA is performed. By reducing the variability in the IDA curves we need fewer records to achieve a given level of confidence in estimating the fractile *IM*-values of limit-state capacities and the mean annual frequencies of limit-state exceedance. Typically, a reduction of the *IM*-capacity dispersion by a factor of two means that we need four times fewer records to gain the same confidence in the fractile *IM*-capacity results (e.g., Vamvatsikos [4]); we could get same quality results by using about eight instead of thirty records. Obviously, the computational savings would be enormous.

Table 1. The suite of thirty ground motion records used.

No	Event	Station	ϕ° ¹	Soil ²	M ³	R ⁴ (km)	PGA (g)
1	Loma Prieta, 1989	Agnews State Hospital	090	C,D	6.9	28.2	0.159
2	Northridge, 1994	LA, Baldwin Hills	090	B,B	6.7	31.3	0.239
3	Imperial Valley, 1979	Compuertas	285	C,D	6.5	32.6	0.147
4	Imperial Valley, 1979	Plaster City	135	C,D	6.5	31.7	0.057
5	Loma Prieta, 1989	Hollister Diff. Array	255	-,D	6.9	25.8	0.279
6	San Fernando, 1971	LA, Hollywood Stor. Lot	180	C,D	6.6	21.2	0.174
7	Loma Prieta, 1989	Anderson Dam Downstrm	270	B,D	6.9	21.4	0.244
8	Loma Prieta, 1989	Coyote Lake Dam Downstrm	285	B,D	6.9	22.3	0.179
9	Imperial Valley, 1979	El Centro Array #12	140	C,D	6.5	18.2	0.143
10	Imperial Valley, 1979	Cucapah	085	C,D	6.5	23.6	0.309
11	Northridge, 1994	LA, Hollywood Storage FF	360	C,D	6.7	25.5	0.358
12	Loma Prieta, 1989	Sunnyvale Colton Ave	270	C,D	6.9	28.8	0.207
13	Loma Prieta, 1989	Anderson Dam Downstrm	360	B,D	6.9	21.4	0.24
14	Imperial Valley, 1979	Chihuahua	012	C,D	6.5	28.7	0.27
15	Imperial Valley, 1979	El Centro Array #13	140	C,D	6.5	21.9	0.117
16	Imperial Valley, 1979	Westmoreland Fire Station	090	C,D	6.5	15.1	0.074
17	Loma Prieta, 1989	Hollister South & Pine	000	-,D	6.9	28.8	0.371
18	Loma Prieta, 1989	Sunnyvale Colton Ave	360	C,D	6.9	28.8	0.209
19	Superstition Hills, 1987	Wildlife Liquefaction Array	090	C,D	6.7	24.4	0.18
20	Imperial Valley, 1979	Chihuahua	282	C,D	6.5	28.7	0.254
21	Imperial Valley, 1979	El Centro Array #13	230	C,D	6.5	21.9	0.139
22	Imperial Valley, 1979	Westmoreland Fire Station	180	C,D	6.5	15.1	0.11
23	Loma Prieta, 1989	Halls Valley	090	C,C	6.9	31.6	0.103
24	Loma Prieta, 1989	WAHO	000	-,D	6.9	16.9	0.37
25	Superstition Hills, 1987	Wildlife Liquefaction Array	360	C,D	6.7	24.4	0.2
26	Imperial Valley, 1979	Compuertas	015	C,D	6.5	32.6	0.186
27	Imperial Valley, 1979	Plaster City	045	C,D	6.5	31.7	0.042
28	Loma Prieta, 1989	Hollister Diff. Array	165	-,D	6.9	25.8	0.269
29	San Fernando, 1971	LA, Hollywood Stor. Lot	090	C,D	6.6	21.2	0.21
30	Loma Prieta, 1989	WAHO	090	-,D	6.9	16.9	0.638

¹ Component ² USGS, Geomatrix soil class ³ moment magnitude ⁴closest distance to fault rupture

Additionally, it is speculated that increasing the efficiency of the *IM*, may also lead to improved *sufficiency* as well. A sufficient *IM* produces the same distribution of demands and capacities independently of the record selection, e.g., there is no bias in the fractile *IM*-capacities if we select records with low rather than high magnitudes or if the records do or do not contain directivity pulses (Luco [6, 7]). The goals of efficiency and sufficiency are not necessarily tied together as the former aims at reducing the variability in the IDA results while the latter at reducing (or eliminating) their dependance on record characteristics other than the *IM*. Still, using a more efficient *IM* will bring the results from all records closer, and similarly bring close the IDA curves of records coming from different magnitudes or containing different directivity pulses, thus reducing the importance of any magnitude or directivity dependance.

While $S_a(T_1, 5\%)$ is found to be both efficient and sufficient for first-mode-dominated, moderate period structures when directivity is not present (Shome [8]), it is not necessarily so for other cases (Luco [6, 7]). Therefore, it is important to try and improve our *IMs* beyond the capabilities of $S_a(T_1, 5\%)$. Figure 2 may provide some clues; therein we have plotted the 5%-damped acceleration spectra of thirty records, chosen to represent a scenario earthquake and appearing in Table 1. The spectra have been normalized by $S_a(2.4s, 5\%)$, i.e., the value of $S_a(T_1, 5\%)$ at the first-mode period $T_1 = 2.4s$ of the 9-story building that we are using as

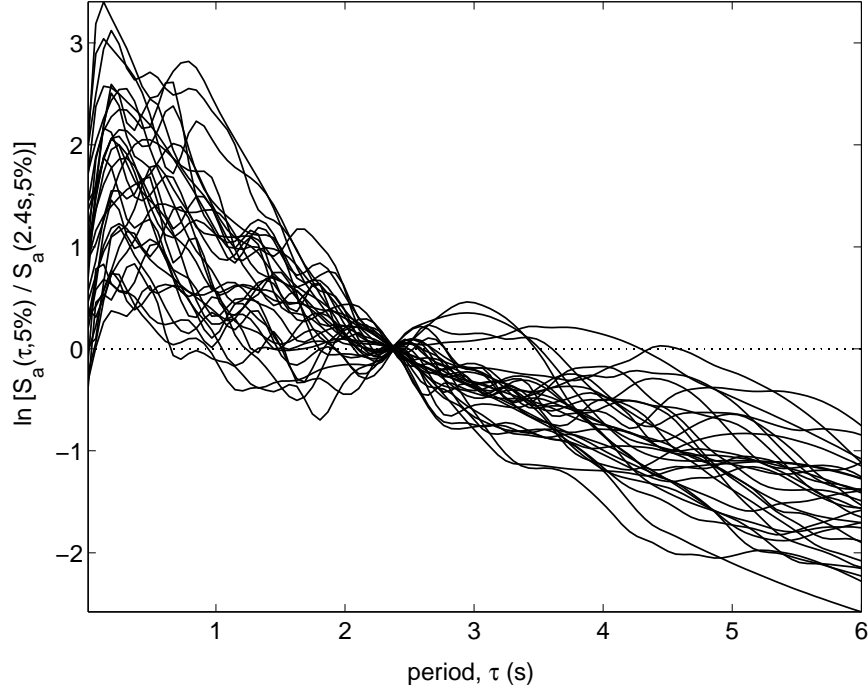


Figure 2. The 5%-damped elastic acceleration spectra for the thirty records of Table 1, normalized by their value at the first-mode period of the 9-story building.

an example. There is obviously much variability in the individual spectra that cannot be captured by just $S_a(T_1, 5\%)$. A structure is not always dominated by a single frequency, and even then, when the structure sustains damage its properties change. Thus, spectral regions away from the elastic first-mode period, T_1 , may become more influential. By taking the differences in the individual spectral shapes into account, we may be able to reduce the variability in the IDA curves and come up with an overall better *IM*.

Such information may be incorporated into the *IM* by using appropriate inelastic spectral values (Luco [6, 7]). This seems to be a promising method, as it directly incorporates the influence of the record on an oscillator that can yield and experience damage in a way similar to the structure. Still, in the context of PBEE, the use of inelastic spectral values requires new, custom-made attenuation relationships. On the other hand, using the elastic spectral values allows the use of the attenuation laws available in the literature. Therefore, there is still much to be gained from the use of *IMs* based on elastic spectra.

Actually, studies by Shome [8], Carballo [9], Mehanny [10] and Cordova [11] have shown that the elastic spectral shape can be a useful tool in determining an improved *IM*. Shome [8] found that the inclusion of spectral values at the second-mode period (T_2) and at the third-mode (T_3), namely $S_a(T_2, 5\%)$ and $S_a(T_3, 5\%)$, significantly improved the efficiency of $S_a(T_1, 5\%)$ for tall buildings. Carballo [9] observed greatly reduced variability in the *DM* demands when spectral shape information was included by compatibilizing a suite of records to their median elastic spectrum. In addition, Mehanny [10] and Cordova [11] observed an improvement in the efficiency of $S_a(T_1, 5\%)$ when an extra period, longer than the first-mode was included by employing an *IM* of the form $S_a(T_1, 5\%)^{1-\beta} S_a(c \cdot T_1, 5\%)^\beta$ (with suggested values $\beta = 0.5$, $c = 2$). Additionally, they presented some evidence suggesting that sufficiency may be improved as well, since the new *IM* made the IDA curves of several near-fault records practically indistinguishable, regardless of the directivity-pulse period. Motivated by such encouraging results, we are going to use the methodology and

tools developed by Vamvatsikos [1, 4] to better investigate the potential of incorporating elastic spectral shape information to *IMs* to reduce the dispersion in IDA results.

METHODOLOGY

For our investigation into the potential use of the elastic acceleration spectrum we have chosen a centerline model of a 9-story steel moment-resisting frame with fracturing connections designed for Los Angeles according to the 1997 NEHRP provisions (Lee [12]). The model incorporates ductile members, shear panels and realistically fracturing Reduced Beam Section connections, while it includes the influence of interior gravity columns and a first-order treatment of global geometric nonlinearities (P- Δ effects). Essentially, it is a first-mode-dominated structure that has its fundamental mode at a period of $T_1 = 2.4$ sec, accounting for 84.3% of the total mass, hence allowing for significant sensitivity to higher modes.

To perform IDA we used the suite of thirty records representing a scenario earthquake, as introduced earlier in Table 1. These belong to a bin of relatively large magnitudes of 6.5 – 6.9 and moderate distances, all recorded on firm soil and bearing no marks of directivity (Vamvatsikos [13]). Each of these records was appropriately scaled to cover the entire range of structural response, from elasticity, to yielding, and finally global dynamic instability. At each scaling level a nonlinear dynamic analysis was performed and a single scalar, the Damage Measure (*DM*), in our case θ_{\max} , was used to describe the structural response. The scaling level and the associated ground motion intensity can be expressed by the selected *IM*, which will initially be $S_a(T_1, 5\%)$ for our investigation. By interpolating such pairs of $S_a(T_1, 5\%)$ and θ_{\max} values for each individual record we get the thirty continuous IDA curves shown in Figure 1b.

While usually only a handful of distinct limit-states of practical value would be defined on the IDA curves (e.g., Immediate Occupancy or Collapse Prevention in FEMA [2, 3]), we will proceed to define numerous limit-states: They will be at given θ_{\max} values to represent the capacity of the structure at successive damaged states and levels of response. Finally, the appropriate $S_a^c(T_1, 5\%)$ -values will be calculated, i.e., the values of $S_a(T_1, 5\%)$ -capacity for each record and each limit-state. Our ultimate goal is to minimize the dispersion in the *IM*-values of capacities for each limit-state *individually* by selecting appropriate spectral values or functions of spectral values to be the *IM*. As a measure of the dispersion we will use the standard deviation of the logarithm of the *IM*-capacities, which is a natural choice for values that are approximately lognormally distributed (e.g., Shome [8]).

Fortunately, no further dynamic analyses are needed to change from $S_a(T_1, 5\%)$ to other *IMs* and perform this dispersion-minimization; all we need to do is to transform each limit-state's $S_a^c(T_1, 5\%)$ -values in the coordinates of the trial *IMs* and calculate their new dispersion. For example, if we want the dispersion of the capacities in PGA terms, then for each unscaled record (or at a scale factor of one) we know both the PGA and $S_a(T_1, 5\%)$ -values and the former can be appropriately scaled by the same factor that the value of $S_a^c(T_1, 5\%)$ implies; e.g., for the 9-story building, the unscaled record #5 (Table 1) has $S_a(T_1, 5\%) = 0.114$ g and PGA = 0.279g, while global instability occurs at $S_a^c(T_1, 5\%) = 0.49$ g, representing a scale factor of $0.49/0.114 \approx 4.3$. Hence, the *IM*-capacity at the global instability limit-state in PGA terms is $\text{PGA}^c = 4.3 \cdot 0.279 = 1.20$ g. Similarly we can accomplish such transformations for any *IM* based on elastic spectral values. Thus, we are taking full advantage of the observations in Vamvatsikos [4], by appropriately postprocessing the existing dynamic runs instead of performing new ones.

The adopted approach in evaluating the candidate *IMs* is very different from the one used by Shome [8], Mehanny [10], Cordova [11] and Luco [6]. There, the focus is on demands, i.e., *DM*-values, all four studies looking for a single “broad-range” *IM* that will improve efficiency for all damage levels of a given structure.

On the other hand, our search will be more focused, zeroing on each limit-state separately to develop a “narrow-range” *IM* that will better explain the given limit-state rather than all of them. Thus, we are able to follow the evolution of such *IMs* as damage increases in the structure, hopefully gaining valuable intuition in the process. Still, since we use only θ_{\max} to define the structural limit-states, our observations may or may not be applicable when limit-states are defined on other structural response measures (e.g., peak floor accelerations).

The focus of our investigation will be on the efficiency gained by incorporating elastic spectrum information in the *IM*. We will start by investigating single spectral coordinates. This does not constitute an investigation of spectral *shape* per se as it focuses on the use of just one value at one period. Still, it will provide a useful basis as we later expand our trial *IMs* to include scalar combinations of two or three spectral values. Another important issue will be the robustness offered by each *IM*, i.e., how much efficiency it retains when the user selects spectral values other than those chosen by the dispersion-minimization process. This is a key question when trying to identify *a priori* an appropriate *IM* in order to take advantage of its efficiency and use fewer records in the analysis. We are not aiming to provide the final answer for the best *a priori* *IM*, but rather to investigate the efficiency and the potential for practical implementation offered by several promising candidates.

USING A SINGLE SPECTRAL VALUE

The use of a single spectral value, usually at the first-mode of the structure, i.e., $S_a(T_1, 5\%)$, has seen widespread use for IDAs, having being incorporated into the FEMA [2, 3] guidelines and used throughout most of our research. Obviously, it is an accurate measure for SDOF systems or first-mode-dominated structures in the elastic range. However, when higher modes are important or the structure deforms into the nonlinear range, it may not be optimal. There seems to be a consensus that when structures are damaged and move into the nonlinear region, period lengthening will occur (e.g., Cordova [11]). In that sense, there may be some merit in looking for elastic spectral values at longer, or in general different, periods than the first-mode. Therefore we will conduct a search, across all periods in the spectrum, to determine the one that most reduces the variability in the *IM*-values of limit-state capacities.

Some representative results for the 9-story building are presented in Figure 3, for the limit-states appearing in Figure 4 at θ_{\max} equal to 0.5% (elastic), 5% (inelastic), 10% (close to global collapse) and $+\infty$ (global instability). The building has significant higher modes, as evident in Figure 3a, since the first mode is not optimal even in the elastic region. While all three modes, T_1 , T_2 and T_3 , seem to locally produce some dispersion reduction, the overall best single period τ is somewhere between T_1 and T_2 , at $\tau \approx 1.2$ s. As the structure becomes progressively more damaged, the optimal period lengthens to higher values, to finally settle close to T_1 when global instability occurs. Actually, there is a whole band of periods around the optimal τ , from 1.1s to 1.7s, that will display low dispersions. As we move away from elasticity and closer to global collapse, this band around the optimal period increases in width and migrates to higher periods as well so that practically any period from 1.7s to 2.5s will achieve relatively low dispersion when close to collapse.

In Figure 5 the results are summarized for all limit-states, showing the gradual lengthening of the optimal period, from $\tau = 1.2$ s in the elastic range up to about $\tau = 2$ s when global collapse occurs. Similarly, in Figure 6 the optimal dispersion thus achieved is compared versus the results when using PGA and $S_a(T_1, 5\%)$. As expected, PGA is the worst choice for any limit-state, while the optimal spectral ordinate is clearly the best of the three. For all three *IMs* the dispersion generally increases as the building accumulates damage but while it does so in a gradual manner for PGA and for the optimal ordinate, this is not the case for $S_a(T_1, 5\%)$.

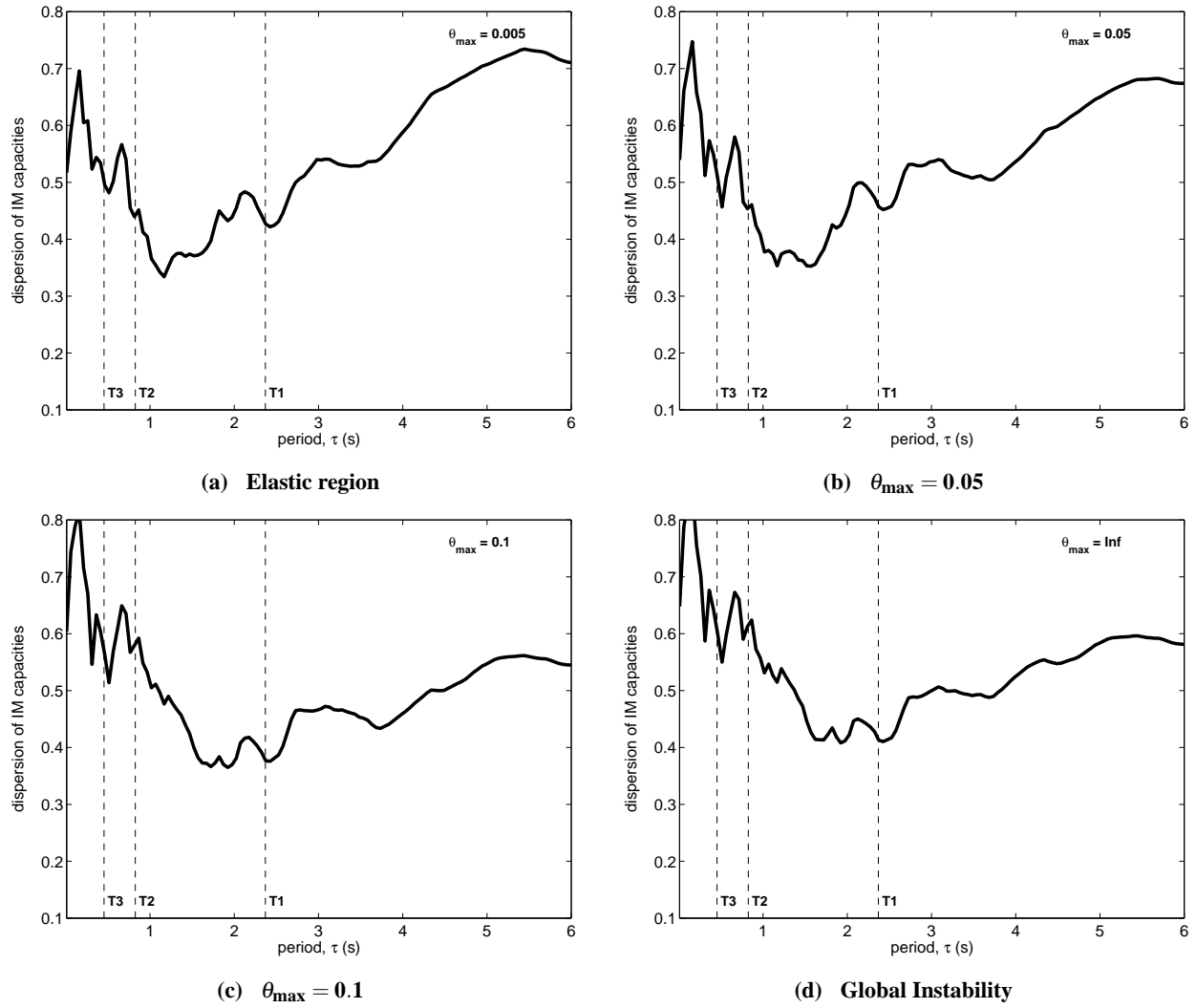


Figure 3. Dispersion of the $S_a^c(\tau, 5\%)$ values versus period τ for four different limit-states for the 9-story building.

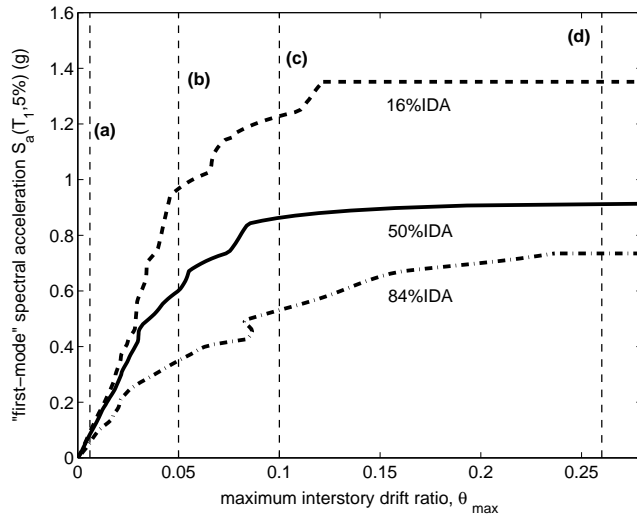


Figure 4. The fractile IDA curves and capacities for four limit-states (Figure 3) of the 9-story building.

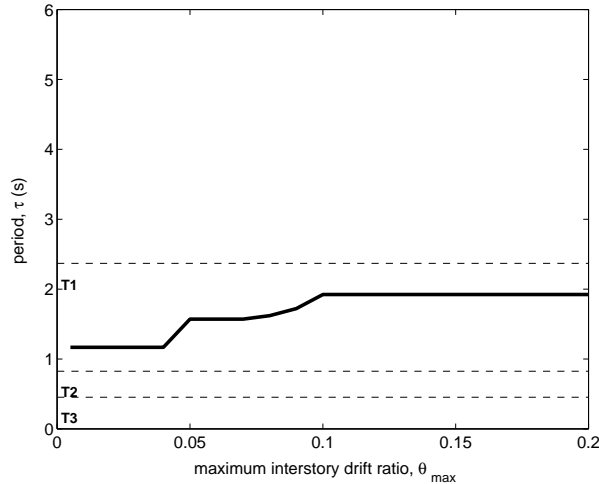


Figure 5. The optimal period, τ , as it evolves for different limit-states defined by θ_{\max} .

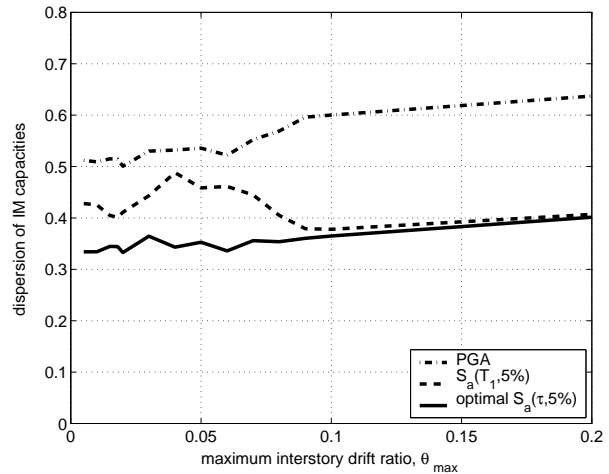


Figure 6. The dispersion when using the optimal $S_a(\tau, 5\%)$ compared to $S_a(T_1, 5\%)$ and PGA, versus the limit-state definition, θ_{\max} .

While $S_a(T_1, 5\%)$ offers dispersions in the order of 45 – 50% for the elastic and most of the inelastic region, it appears to become almost optimal when the building approaches collapse. Thus, only in the elastic and near-elastic region does the single optimal spectral value provide improved dispersion reduction, in the order of an additional 10%. Close to global collapse, no significant gains are realized over $S_a(T_1, 5\%)$.

Summarizing our observations, the use of a single optimal spectral value seems to offer some benefits achieving some dispersion reduction especially in the elastic and near-elastic region for this 9-story building. Although some single optimal period exists for such first-mode dominated structures and it predictably lengthens as the structure accumulates damage, it may not be so easy to identify. There does exist a certain band of periods around the optimal that would provide us with good results, but how is one to choose appropriately when the useful band of periods seems to lie somewhere between T_2 and T_1 , moving from the former to the latter as damage increases? This might be an easier task for buildings with less influence from higher modes, but for this 9-story, where higher modes are indeed present, one spectral value is probably not enough. It would be difficult to pick *a priori* a single period for such a structure as a bad guess could penalize the dispersion considerably, producing worse results than $S_a(T_1, 5\%)$.

Most probably, the reason behind this apparent difficulty is that both in the elastic and in the nonlinear range the structure is sensitive to more than one frequencies. Thus, our attempt to capture this effect with just one period results in the selection of some arbitrary spectral coordinate that happens to provide the right “mix” of spectral values at the significant frequencies. Looking at all the previous figures, it becomes obvious that missing by a little will again, in most cases, pump up the dispersion significantly. Obviously, this one period is not a viable solution for structures that are not completely dominated by the first-mode. On the other hand, the introduction of additional spectral values, to form a vector or an appropriate scalar combination of two or more periods, might prove better.

USING A POWER-LAW FORM WITH TWO OR THREE SPECTRAL VALUES

Incorporating more than one spectral ordinate into our candidate *IM* can be done in two ways: Either by creating a vector of spectral values or by combining them into a single scalar quantity. The use of vector *IMs* has been explored by Vamvatsikos [13] but in our current spectral shape investigation we choose to

focus only on scalar combinations of spectral values and in particular the use of a power law form.

Not surprisingly, it is such a form that Shome [8], Mehanny [10] and Cordova [11] have used to create a new, more effective scalar *IM*. While the idea there was mostly driven by the need to be able to use existing attenuation laws to create hazard curves for the new *IM* (Cordova [11]), the work done on vector *IMs* by Vamvatsikos [13] provides some clues as to why such forms may achieve significant efficiency.

Formally, we intend to perform a search for the optimally efficient *IM* of the form

$$\begin{aligned} IM &\equiv S_a(\tau_a, 5\%)^{1-\beta} S_a(\tau_b, 5\%)^\beta \\ &= S_a(\tau_a, 5\%) \left[\frac{S_a(\tau_b, 5\%)}{S_a(\tau_a, 5\%)} \right]^\beta \end{aligned} \quad (1)$$

where τ_a and τ_b are arbitrary periods and $\beta \in [0, 1]$. Notice the difference with Shome [8] who constrains both periods to be T_1 and T_2 respectively, or Mehanny [10] and Cordova [11], who chose to constrain one of the periods to be T_1 . Instead, we intend to let the optimization find the best values, τ_a , τ_b and β .

Additionally, we will investigate a power-law form containing three spectral values or, equivalently, a single spectral value and two spectral ratios:

$$\begin{aligned} IM &\equiv S_a(\tau_a, 5\%)^{1-\beta-\gamma} S_a(\tau_b, 5\%)^\beta S_a(\tau_c, 5\%)^\gamma \\ &= S_a(\tau_a, 5\%) \left[\frac{S_a(\tau_b, 5\%)}{S_a(\tau_a, 5\%)} \right]^\beta \left[\frac{S_a(\tau_c, 5\%)}{S_a(\tau_a, 5\%)} \right]^\gamma \end{aligned} \quad (2)$$

where τ_a , τ_b and τ_c are arbitrary periods, $\beta, \gamma \in [0, 1]$ and $\beta + \gamma \leq 1$.

The optimal two periods for the 9-story building appear in Figure 7 over a range of limit-states from elasticity to global collapse. In elasticity, the two periods τ_a and τ_b actually coincide with the first and second mode periods, T_1 and T_2 , respectively. As damage increases, one of the periods hovers slightly higher than T_2 , while the other stays close to T_1 , increases dramatically to an almost 120% higher value when the structure reaches $\theta_{\max} = 6\%$, but then it drops again to values somewhat higher than T_1 when close to global collapse. The optimal value of β is always about 0.5, favoring equal weighting of the two periods.

The optimal dispersion achieved with two spectral ordinates is plotted again versus the dispersion when using PGA and $S_a(T_1, 5\%)$ in Figure 8. Comparing Figures 6 and 8 it becomes obvious that the use of two spectral values reduces the capacity dispersion by a significant amount relative to the use of a single (optimal) value for all limit-states. Actually, the dispersion drops from 40% for one optimal period (or even for just $S_a(T_1, 5\%)$), to less than 25 – 30% when two periods are used.

If we introduce a third spectral value for the 9-story through Equation 2, then we come up with the three optimal periods shown in Figure 9 for a range of damage-states. In the regions of elasticity and early inelasticity, the three optimal periods τ_a , τ_b and τ_c remain close to the first three modes, T_1 , T_2 and T_3 . When θ_{\max} reaches approximately 4% the optimal periods suddenly increase. Then, the results seem to favor one period at about twice T_1 , another at T_1 and a third at T_2 . Again, equal weighting seems to be the rule for all limit-states since the optimal values are $\beta \approx \gamma \approx 1/3$.

With either two or three periods, as seen when comparing Figures 8 and 10, the dispersion reduction is about the same; using three instead of two optimal periods allows only an additional decrease of 1 – 4%. It seems that two spectral values are enough for this first-mode-dominated building and clearly better than just one,

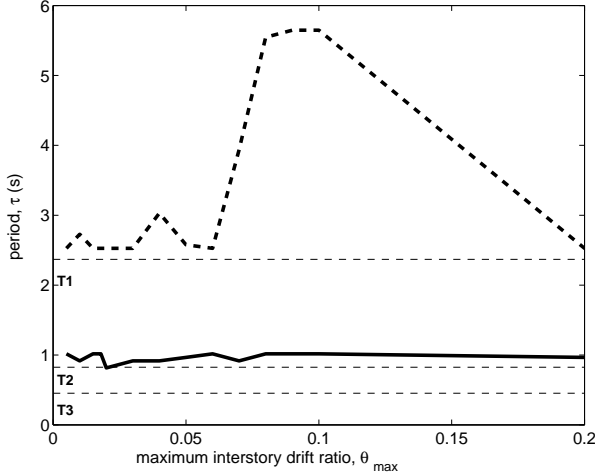


Figure 7. The two optimal periods τ_a , τ_b as they evolve with θ_{\max} .

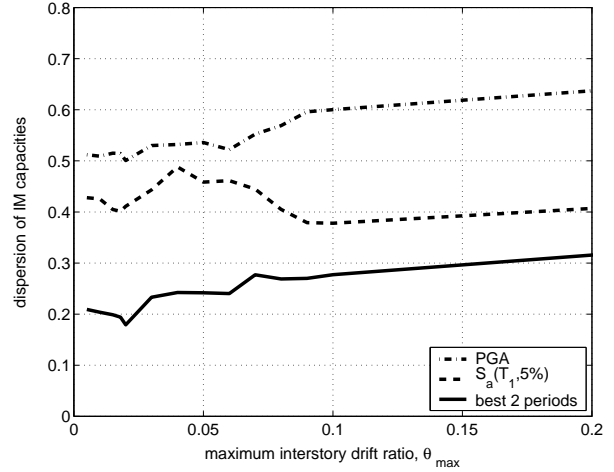


Figure 8. The dispersions for the 9-story building when using PGA or $S_a(T_1, 5\%)$ versus the optimal $S_a(\tau_a, 5\%)^{1-\beta} S_a(\tau_b, 5\%)^\beta$.

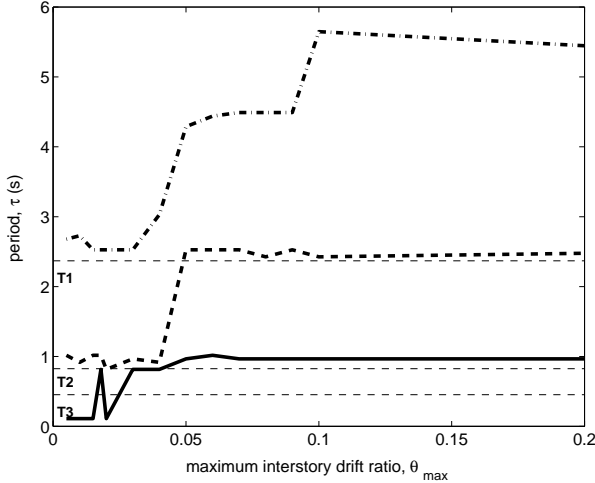


Figure 9. The three optimal periods τ_a , τ_b , τ_c as they evolve with θ_{\max} .

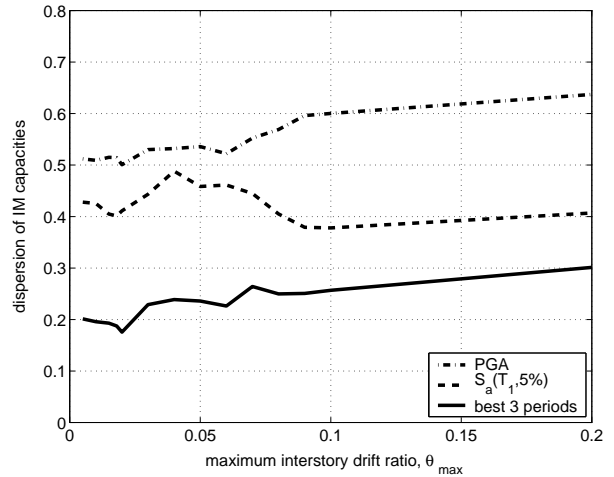


Figure 10. The dispersions for the 9-story building for PGA and $S_a(T_1, 5\%)$ versus the optimal $S_a(\tau_a, 5\%)^{1-\beta-\gamma} S_a(\tau_b, 5\%)^\beta S_a(\tau_c, 5\%)^\gamma$.

but the use of three carries a distinct advantage: Their behavior is more stable and predictable than the case of the two periods, i.e., they seem easier to identify.

When practically implementing such *IMs* before the dynamic analyses are performed, it is important that efficiency remains high even when not using the (unknown *a priori*) optimal periods. To investigate the sensitivity of the proposed scalar *IMs* we have simulated random user choices for the period(s) used for the single spectral value or the power-law combinations of two or three values. The user is supposed to have picked periods uniformly distributed within $\pm 20\%$ of the optimal values for each *IM* and to have selected equal weighting of spectral values in the power-law (i.e., $\beta = 1/2$ or $\beta = \gamma = 1/3$). Such simulations are repeated numerous times for each limit-state (i.e., value of θ_{\max}) and the achieved suboptimal dispersion is calculated for each *IM*. In Figure 11 we are plotting the 84%-fractile of the suboptimal dispersion for the single period and the two power-law combinations versus the θ_{\max} definition of each limit-state; i.e., we are focusing on a worse-than-average scenario. For comparison, the dispersion when using $S_a(T_1, 5\%)$ and when using the optimal three periods power-law is also shown.

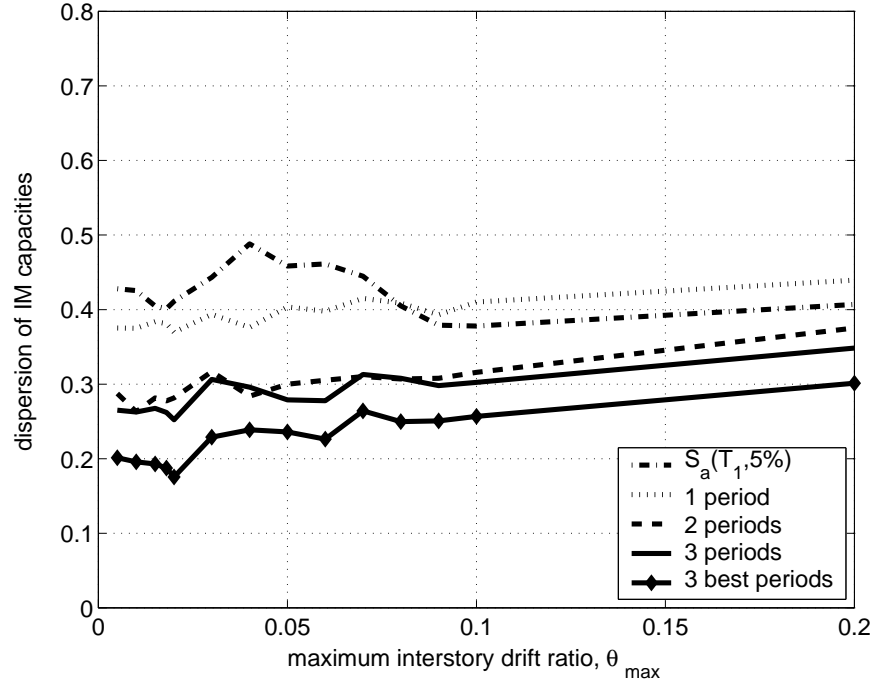


Figure 11. The 84% fractile of the suboptimal dispersion when using a single spectral value versus a power-law combination of two or three periods for the 9-story building. For comparison, the dispersion achieved by $S_a(T_1, 5\%)$ and the optimal three-periods power-law is also shown.

Clearly, using only one (suboptimal) period is often worse or at most as good as when using $S_a(T_1, 5\%)$, as originally observed in Figure 3. On the other hand, with two, or even better, three periods, equally weighted in a power-law form, the *IM* is considerably more robust and relatively reasonable efficiency is maintained. If we follow our earlier observations and set one value around T_1 , another at about T_2 and maybe a third 50% or 100% higher than T_1 , then weigh them equally ($\beta = 1/2$ or $\beta = \gamma = 1/3$), a dispersion of about 30% (down from about 40 – 50% when using $S_a(T_1, 5\%)$) is easily achieved in contrast to the elusive single optimal period. In conclusion, it seems that the use of the power-law form with two or three spectral values helps even when the higher modes are significant. The benefit is not so much in the reduction of dispersion, rather in the robustness of the *IM* and the ability to identify it *a priori*. Further investigation of more structures is needed before some concrete proposals are made, but the concept looks promising.

CONCLUSIONS

Providing more efficient Intensity Measures (*IMs*) is a useful exercise, both in reducing the number of records needed for PBEE calculations but also in improving our understanding of the seismic behavior of structures. By taking advantage of elastic spectrum information the observed record-to-record dispersion was nearly halved for some limit-state *IM*-capacities of the investigated 9-story building. While several methods exist to incorporate elastic spectral values in *IMs* we only focused on the use of single optimally-selected spectral values and power-law combinations of two or three optimal spectral values. Not all candidates can achieve similar degrees of efficiency and not all of them are suitable for use *a priori*; it may be quite difficult to select the appropriate periods (or spectral values) before we complete our dynamic analyses. Using a single optimal spectral value does not seem to provide much advantage for the 9-story building

as it has some higher-mode influence. However, spectral *shape* is important: using two or even three spectral values seems to improve the efficiency but also the robustness of the *IM* to the suboptimal selection of periods. Still, before such *IMs* are adopted significant work remains to be done; we need to investigate more structures, both with less and more higher mode influence and more ground motion records, probably ones with important local spectral features, e.g., soft soil or directivity influence. Thus we will be able to better select the appropriate *IM* that will be both efficient and sufficient for a given structure and site.

ACKNOWLEDGMENTS

Financial support for this research was provided by the sponsors of the Reliability of Marine Structures Affiliates Program of Stanford University.

REFERENCES

1. Vamvatsikos D, Cornell CA. "Incremental dynamic analysis." *Earthquake Engineering and Structural Dynamics* 2002; 31(3): 491–514.
2. FEMA. "Recommended seismic design criteria for new steel moment-frame buildings." Report No. FEMA-350, SAC Joint Venture, Federal Emergency Management Agency, Washington DC, 2000.
3. FEMA. "Recommended seismic evaluation and upgrade criteria for existing welded steel moment-frame buildings." Report No. FEMA-351, SAC Joint Venture, Federal Emergency Management Agency, Washington DC, 2000.
4. Vamvatsikos D, Cornell CA. "Applied incremental dynamic analysis." *Earthquake Spectra* 2004; 20(2).
5. Vamvatsikos D, Cornell CA. "Direct estimation of the seismic demand and capacity of oscillators with multi-linear static pushovers through incremental dynamic analysis." *Earthquake Engineering and Structural Dynamics* 2004; In review.
6. Luco N, Cornell CA. "Structure-specific, scalar intensity measures for near-source and ordinary earthquake ground motions." *Earthquake Spectra* 2004; In review.
7. Luco N. "Probabilistic seismic demand analysis, SMRF connection fractures, and near-source effects." PhD Dissertation, Department of Civil and Environmental Engineering, Stanford University, Stanford, CA, 2002. URL http://www.stanford.edu/group/rms/Thesis/Luco_Dissertation.zip. (accessed: Feb 12th, 2004).
8. Shome N, Cornell CA. "Probabilistic seismic demand analysis of nonlinear structures." Report No. RMS-35, RMS Program, Stanford University, Stanford, CA, 1999. URL <http://www.stanford.edu/group/rms/Thesis/NileshShome.pdf>. (accessed: Feb 12th, 2004).
9. Carballo JE, Cornell CA. "Probabilistic seismic demand analysis: Spectrum matching and design." Report No. RMS-41, RMS Program, Stanford University, Stanford, CA, 2000. URL <http://www.stanford.edu/group/rms/Reports/RMS41.pdf>. (accessed: Feb 12th, 2004).
10. Mehanny SS, Deierlein GG. "Modeling and assessment of seismic performance of composite frames with reinforced concrete columns and steel beams." Report No. 136, The John A. Blume Earthquake Engineering Center, Stanford University, Stanford, CA, 2000.
11. Cordova PP, Deierlein GG, Mehanny SS, Cornell CA. "Development of a two-parameter seismic intensity measure and probabilistic assessment procedure." *Proceedings of the 2nd U.S.-Japan Workshop on Performance-Based Earthquake Engineering Methodology for Reinforced Concrete Building Structures*. Sapporo, Hokkaido, 2000, 187–206.

12. Lee K, Foutch DA. "Performance evaluation of new steel frame buildings for seismic loads." *Earthquake Engineering and Structural Dynamics* 2002; 31(3): 653–670.
13. Vamvatsikos D. "Seismic performance, capacity and reliability of structures as seen through incremental dynamic analysis." PhD Dissertation, Department of Civil and Environmental Engineering, Stanford University, Stanford, CA, 2002. URL <http://www.stanford.edu/group/rms/Thesis/Dimitrios-1side.pdf>. (accessed: Feb 12th, 2004).